



Modeling Frictional Characteristics of Water Flowing Through Microchannel

P. C. Jayadevan¹, R. Siddharth² and Pradeep M. Kamath^{1†}

¹ Heat Transfer Research Laboratory, Department of Mechanical Engineering, Government Engineering College, Thrissur, Kerala, India

² R & D Department, Achira Labs Pvt Ltd, Bangalore, Karnataka, India

†Corresponding Author Email: pradeepmkamath@gmail.com

(Received February 21, 2018; accepted August 11, 2018)

ABSTRACT

The present study aims at modeling the real random rough surface of a microchannel with structured rough channel of known geometric parameters. The surface of the microchannel is created by sinusoidal function using MATLAB code and 2D simulation of the model is carried out with commercial software ANSYS Fluent. The height of the channel is varied from 100 to 250 μm and length of the channel is 12.5 mm. The range of Reynolds number selected for analysis is 100 to 500 with water as the fluid medium. The roughness height is selected within the range of actual manufacturing roughness level of microchannels. The results show that channel geometry has significant influence on flow characteristics. A new non-dimensional roughness parameter β , is proposed to represent the dependence of friction factor on geometric parameters in the laminar region. A correlation for flow friction is developed as a function of roughness parameter and Reynolds number.

Keywords: Microchannel; Numerical simulation; Surface roughness; Friction factor; Correlation.

NOMENCLATURE

C	friction coefficient	f	friction factor
e	roughness height	β	roughness parameter
H	channel height	ΔP	pressure drop
H_c	constricted height	l	length of fully developed region
Re	Reynolds number	λ	roughness pitch
W	width of the channel	μ	viscosity of water
x	longitudinal distance from inlet	V	inlet velocity
$Y_l(x)$	equation of lower surface	ρ	density of water
$Y_u(x)$	equation of upper surface	Φ	phase angle, radians

INTRODUCTION

With the development of micro electromechanical systems, microchannels are widely used as passage for heat carrying medium. In 1981, Tuckerman and Pease (1981) experimentally demonstrated high heat sinking capacity of Silicon based microchannels. Since then, many experimental and numerical investigations are carried out to study heat transfer performance of micron scale channels. The unique performance enhancement of microchannel is attributed to its high surface to volume ratio. In the late eighties, the attention was focused on the study of flow characteristics through microchannels.

Pfahler *et al.* (1990) investigated liquid flow through silicon rectangular microchannels. It is found that flow through large channels follows Navier-Stoke equation and small channels exhibit considerable deviation from the classical theory. Friction coefficient obtained is approximately three times higher than the conventional theory whereas at higher Reynolds number it is found to be independent of Reynolds number. Peng *et al.* (1994) experimentally analyzed water flowing through rectangular microchannels having hydraulic diameter ranging from 0.133-0.367 mm. The experiments reveal that the value of friction factor deviates from classical theory in both laminar and

turbulent region. The results showed that the hydraulic diameter and height to width ratio have a significant effect on friction factor. They also observed an early transition for the flow. [Pfund *et al.* \(2000\)](#) studied pressure drop in microchannel using water as working medium and found friction factor is significantly higher than conventional value. The convective heat transfer in trapezoidal silicon microchannels was studied by [Wu and Cheng \(2003\)](#). The experimental data with water showed that friction factor is different from conventional values and depends on geometric parameters like surface roughness and hydrophilic property of the surface. They proposed a dimensionless correlation for apparent friction factor and Nusselt number using their experimental data.

[Wang *et al.* \(2016\)](#) numerically analyzed the influence of geometric parameters on flow characteristics and heat transfer performance of microchannel heat sink by considering the variation of viscosity of water with temperature. The analysis was carried out for rectangular, trapezoidal and triangular microchannels of hydraulic diameter ranging 0.172-0.406 mm and aspect ratio 1.03-20.3. The results revealed that the less the hydraulic diameter the more significant is the pressure drop and narrowly shaped microchannels like trapezoidal and triangular have a high pressure drop compared to the rectangular channel. Also, for the hydraulic diameter of the order of 0.349 mm, the conventional theory can predict the flow characteristics. [Sahar *et al.* \(2017\)](#) numerically investigated the relative importance of hydraulic diameter and aspect ratio on fluid flow through rectangular microchannel. They used two sets of channel dimension, one with aspect ratio 1 and hydraulic diameter varying from 0.1-1 mm and another with hydraulic diameter 0.56 mm and aspect ratio 0.39-10. The analysis carried out for Reynolds number 100-2000 and water was selected as working medium. The results showed that for aspect ratio up to 2, friction factor found to decrease whereas, friction factor increases continuously for all Reynolds numbers for higher aspect ratio. When hydraulic diameter increases, the friction factor is found to increase. The results also revealed that the dimensionless hydrodynamic entry length does not depend on aspect ratio and hydraulic diameter within the limit of Reynolds number selected for analysis.

[Li \(2003\)](#) experimentally analyzed flow characteristics of deionized water through glass, silica and stainless steel microtubes. Flow through glass and silica microtubes follow classical theory. The Poiseuille number for stainless steel microtube exceeds the value corresponding to conventional theory and an early transition reported. [Li *et al.* \(2007\)](#) studied liquid flow and heat transfer in smooth silica and rough stainless steel microtubes numerically and experimentally using deionized water. The results indicate that conventional frictional theory did not hold good in rough stainless steel microtubes and reported a higher value for friction factor. According to experimental data obtained by [Lin *et al.* \(2014\)](#) using air and CO_2 as working fluid, there is an apparent effect of roughness on flow characteristics, but thermal

performance is almost same for both smooth and rough tubes. [Liu *et al.* \(2015\)](#) experimentally investigated the flow characteristics and heat transfer characteristics in stainless steel rectangular microchannels with different surface roughness using air as working medium. The results show that friction factor and the Nusselt number increase with relative roughness and heat flux rarely affects the Nusselt number. [Kim \(2016\)](#) experimentally analyzed fully developed laminar flow through rectangular microchannel using water and FC770 as working fluid. The hydraulic diameter of the channel ranges from 155-580 μm and aspect ratio 0.25-3.8. Experiments revealed that the normalized friction factor is a function of Reynolds number in the laminar region and the value falls between 0.9-1.1. The Poiseuille number for small aspect ratio channels showed a large deviation from theoretical value due to the effect of the roughness of microchannel. [Zhai *et al.* \(2017\)](#) experimentally studied the flow of deionized water through rectangular microchannel of dimension 20mm \times 10mm \times 0.85mm for Reynolds number ranging 130-850. They proposed a theoretical model for apparent friction factor and the model was validated with their experimental data and results available in the literature. [Guo *et al.* \(2015\)](#) numerically analyzed the influence of wall roughness models on fluid flow and heat transfer in microchannels and proposed more efficient and convenient 3D Gauss model to describe fluid flow and thermal performance. The results proved that roughness has a positive effect on friction factor even in the laminar flow region. [Pelevic' and Meer \(2016\)](#) investigated the effect of roughness on fluid flow through microchannels by lattice Boltzmann method. Gauss function was used to create the rough surface and this simplified roughness model was compared with the real random rough model. The results show that the simplified model can be used to mimic the real roughness model. [Mala and Li \(1999\)](#) studied water flow through microtubes numerically and experimentally and proposed a roughness-viscosity model. The effect of roughness on flow is represented by a roughness-viscosity function and is solved using experimental data. The results vary from channel to channel and depend on channel shape and roughness distribution of microchannel.

Since controlling the roughness parameter is very difficult in real systems, many researchers numerically modeled surface roughness with structured geometric shapes and proposed wall roughness models to explain the performance of microchannels. [Kandlikar *et al.* \(2005\)](#) proposed a constricted flow model to characterize the effect of roughness in single phase flow through rectangular microchannels with sawtooth profile. In the laminar region the constricted parameter approach results in good agreement with the theory. Whereas in turbulent region the experimental friction factor is much higher than the theoretical value. The experiments were carried out with constricted relative roughness of 0-0.14 with air and water as working medium. They also proposed a modified Moody diagram based on constricted parameters. [Rawool *et al.* \(2006\)](#) carried out numerical

investigation on the flow through microchannels using rectangular, trapezoidal and triangular roughness elements and proposed a three-dimensional roughness model. The results show that friction factor highly depends upon the shape of the roughness geometry and it decreases with increase in Reynolds number. [Croce *et al.* \(2007\)](#) simulated fluid flow through microchannels designed with conical roughness elements and proposed a correlation to fit the data set. [Zhang *et al.* \(2010\)](#) conducted numerical simulation of fluid flow through microchannels using two dimensional roughness elements. The results show that Poiseuille number and Nusselt number are independent of Reynolds number.

[Wagner and Kandlikar \(2009\)](#) used wall function method with lubrication approximation to analyze the flow through designed transverse rib shaped rectangular microchannel. The wall function method was compared with constricted flow model and found both the models are comparable with those of smooth channels. [Dharaiya and Kandlikar \(2013\)](#) used sinusoidal roughness pattern to model the channel roughness and presented a two dimensional roughness model. The analysis was carried out for aligned configuration for channel height 550 μm , 750 μm and 250 μm . The Reynolds number used for the analysis is 100 and roughness height varied from 10 μm to 100 μm . The pitch of the channel used are 150 μm , 250 μm and 400 μm and found that the pitch doesn't have any significant effect on fully developed Nusselt number. They also found that the structured roughness elements result in an increase in pressure drop and heat transfer characteristics compared to conventional theory. [Wagner and Kandlikar \(2012\)](#) studied effect of two dimensional aligned sinusoidal roughness pattern on microchannel flows experimentally and numerically. The experiments are conducted with roughness height varying from 36-131 μm and Reynolds number 5-3400. The height of the channel is varied from 230-937 μm . A theoretical model is proposed to predict the pressure drop in fully developed laminar flow and validated with experimental data. [Koopae and Zare \(2015\)](#) numerically investigated the effect of aligned and offset sinusoidal roughness pattern on rectangular microchannel flows. The simulations were carried out for Reynolds number 100 and channel height 250-550 μm . The roughness height is varied from 10-100 μm . The results show that at high roughness height offset roughness pattern has low pressure drop compared to the aligned pattern, whereas at low roughness height the difference is insignificant for both configurations.

The review of literature in fluid flow through micron scale passages exhibits a considerable deviation of friction factor from the conventional theory. This deviation is mainly due to the high relative roughness of microchannel compared to macrochannel. Since pumping power is a major parameter for the design of microfluidic devices, finding of friction factor is of paramount importance in the study of microchannel flows. Many researchers studied the effect of roughness on flow friction characteristics. Table 1 represents correlations for friction factor in

laminar flow domain of microchannel. It has been observed that the use of correlation is restricted with reasons like experimental data are essential to evaluate the empirical coefficients, in many cases, the experiments are done with very large roughness value which is out of actual manufacturing roughness level of the microchannel [Weaver *et al.* \(2011\)](#) and some correlations are compared with smooth channel results. Most of the correlations do not involve roughness term explicitly, this is also a major drawback of the existing empirical and analytical models.

Microchannels have high heat sinking capacity and are widely used for cooling of electronic devices and turbine blades of aircrafts [Weaver *et al.* \(2011\)](#). In biotechnology, microchannels are extensively used for the analysis and synthesis of proteins, DNA and chemical reagents [Whitesides \(2006\)](#). Microfluidic technology has emerged as a powerful tool in cell-based research due to its high precision, sensitivity and greater control over the parameters [Zhuang *et al.* \(2016\)](#). Rapid sample processing capability and low fluid volume consumption of microfluidic devices have made them an essential component in the development of lab-on-a-chip devices [Sackmann *et al.* \(2014\)](#) and in-vitro multicellular human organisms [Bein *et al.* \(2018\)](#). Since microchannels are an integral part of microfluidic systems, it is essential to determine the characteristics of fluid flow through micron scale passages for better design of various micro devices. The objective of present study is to develop a correlation for friction factor by modeling the microchannel surface using a sinusoidal function. It is a known fact that entirely different surface profiles can have the same average roughness value, which is a representative of randomness of the surface [Ferreira *et al.* \(2011\)](#). In the present study, numerical simulation is carried out in the laminar region of the flow with sinusoidal rough surface. The roughness height is chosen within manufactured roughness level of microchannels and simulation is carried out at different Reynolds numbers.

NUMERICAL MODEL

Numerical analysis is carried out for channel height varying 100 - 250 μm by selecting roughness height within actual roughness value of microchannels.

The range of Reynolds number selected for the analysis is 100 - 500 to ensure the laminar flow conditions. Since many experiments ([Kandlikar *et al.* \(2005\)](#), [Wagner and Kandlikar \(2012\)](#), [Brackbill and Kandlikar \(2007\)](#) and [Hao *et al.* \(2006\)](#)) revealed that transition might occur at Reynolds number as small as 570. The 2D geometry of the model is adapted from [Wagner and Kandlikar \(2012\)](#). The bottom and top walls of the surface are defined with sinusoidal functions and can be expressed respectively as,

$$Y_l(x) = e \times \cos^4 \frac{\pi x}{\lambda} \quad (1)$$

Table 1 Friction factor correlations for laminar flow through microchannel

Authors	Geometry	Correlation	Remarks
Pfahler <i>et al.</i> (1990)	Rectangular, n-propanol, A_c -80-7200 μm^2	$f = \frac{C}{Re}$	C ,friction coefficient of the system depends on channel geometry and independent of Re
Peng <i>et al.</i> (1994)	Rectangular, Water, D_H -0.133-0.367 μm , Re - 50-4000	$f = \frac{C_f}{Re^{1.98}}$	C_f -empirical coefficient
Wu and Cheng (2003)	Trapezoidal, Water, $\frac{L}{D_H}$ - 285-451, Re - 10-1500	$f_{app} Re = C_3 Re^{0.089} \times (1 - \frac{W_b}{W_t})^{4.359} \times (\frac{W_t}{H})^{4.444} \times (\frac{k}{D_h})^{0.028} \times (\frac{D_h}{2})^{1.023}$	$0 \leq \frac{w_b}{w_t} \leq 0.934$, $0.038 \leq \frac{H}{W_t} \leq 0.648$, $3.28 \leq \frac{k}{D_h} \leq 1.09 * 10^{-2}$, $191.77 \leq \frac{L}{D_h} \leq 453.79$, C_3 -correlation factor depends on surface material, W_t and W_b - bottom and top width of microchannel, $\frac{k}{D_h}$ -relative roughness
Liu <i>et al.</i> (2015)	Rectangular, air, Re - 200-2100, 0.4×0.4 mm	$f Re = 77.24 \varepsilon^{0.163} + (0.027 - 0.2 \exp(\frac{-\varepsilon}{0.00223}))$	ε -roughness height
Zhai <i>et al.</i> (2017)	Rectangular, deionized water, $20mm \times 10mm \times 0.85mm$, Re -130-850	$f_{app} = \frac{\Delta PD_h}{2\rho u_m^2 L_{ch}}$	L_{ch} - Channel height, u_m -mean velocity
Dharaiya and Kandlikar (2013)	Rectangular, Sinusoidal roughness, Water, H -550 μm , Re -100, λ - 250 and 150 μm , e =50 μm	$f_{cf} = \frac{dP}{dx} \frac{\rho D_{h,cf} A_{cf}^2}{2rh^2}$	Constricted model, cf denotes constricted parameters, \dot{m} - mass flow rate, A_{cf} - constricted area
Hsieh <i>et al.</i> (2004)	Rectangular, deionized water, D_h -146 μm	$f = 48.1 Re^{-0.94}$ $Re < 240$	Transition reported at $Re \approx 240$
Mala and Li (1999)	Circular, water	$\frac{\mu_k}{\mu} = A Re \frac{y}{k} (1 - \exp(\frac{Re_k y}{Re k}))$	Roughness Viscosity model, A - coefficient determined from experimental data which depends on channel shape, Re_k -roughness Reynolds number, μ_k - roughness viscosity
Peiyi and Little (1983)	Trapezoidal, Nitrogen, D_h - 55-76 μm , $Re < 900$	$f = \frac{110 \pm 8}{Re}$	transition reported at $Re \approx 400$
Kakac, <i>et al.</i> (1987)	Rectangular	$f = \frac{24}{Re} (1 - 1.3553\alpha + 1.9467\alpha^2 - 1.7012\alpha^3 + 0.9564\alpha^4 - 0.2537\alpha^5)$	Smooth channel, aspect ratio $\alpha < 1$
White (2011)	flow between parallel plates	$f = \frac{96}{Re D_h}; \pm 33\%$	Macrochannel flow, fRe_{D_h} depends on aspect ratio
Yu <i>et al.</i> (1995)	Circular, Nitrogen and Water, D =19, 52, 102 μm , $Re < 2000$	$f = 50.13/Re$	D =Diameter of tube
Choi <i>et al.</i> (1991)	Circular, Nitrogen, D - 3-81 μm , $Re < 2000$	$f = \frac{64}{Re} [1 + 30(\frac{v}{Dc_a})]^{-1}$	D = Diameter, c_a -empirical constant
White (2011)	Circular	$f = \frac{64}{Re_{D_h}}; \pm 40\%$	Macrochannel flow

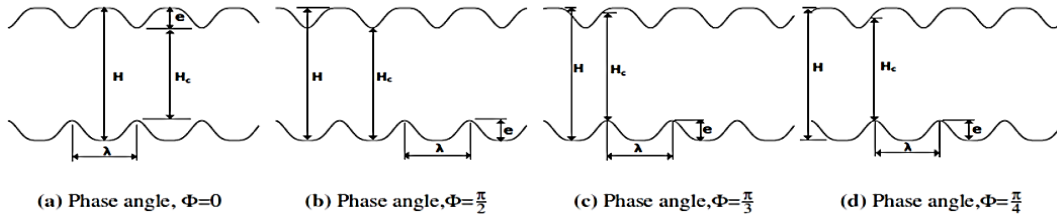


Fig. 1. 2D geometry of the microchannel for different phase angle.

$$Y_u(x) = H - e \times \cos^4\left(\frac{\pi x}{\lambda} + \Phi\right) \quad (2)$$

where, H is the channel height, e and λ define roughness height and roughness pitch respectively, x is the longitudinal distance from the inlet and Φ is phase angle. The value of phase angle defines the amount of offset between peaks of upper and lower surfaces. The geometry of the model considered for the analysis is shown in Fig. 1, and Table 2 describes the parameters used for creating the model.

Table 2 Geometric parameters used for numerical analysis

$e(\mu m)$	$H(\mu m)$	$\lambda(\mu m)$	Φ
5, 10, 15, 20, 25, 30	250	250	$0, \frac{\pi}{2}, \frac{\pi}{3}, \frac{\pi}{4}$
1, 5, 10	200	200	$0, \frac{\pi}{2}$
1, 3, 5	160	160	$0, \frac{\pi}{2}$
1, 2, 3, 4, 5	100	100	$0, \frac{\pi}{2}$

In the present study, commercial software package ANSYS Fluent is used to simulate the flow through microchannel with water as working medium. The assumptions used for the analysis are (1) steady, laminar, incompressible flow, (2) constant physical properties and (3) no-slip condition at the wall. The numerical study of Guo *et al.* (2015) reveals that no-slip velocity condition is a reasonable assumption for modeling fluid flow over the structured rough surface.

The governing equations used to solve the model are,

Conservation of mass:

$$\nabla U = 0 \quad (3)$$

Conservation of momentum:

$$(U \cdot \nabla) \rho U = -\nabla P + \mu \nabla^2 U \quad (4)$$

where, U is the velocity vector, P is the pressure, ρ and μ are density and dynamic viscosity of the fluid respectively. The boundary conditions specified are, constant uniform velocity at inlet and ambient pressure at the outlet.

MATLAB code is developed to generate the geometries with parameters specified by Table 2 in ANSYS Fluent design modular interface and is

meshed with ANSYS mesh module. Figure 2 represents the schematic of the mesh geometry for channel height $250 \mu m$ and roughness height $20 \mu m$.

The grid independence study of the model is conducted for all geometries and optimum number of nodes for the analysis is obtained. Residual of $10E-12$ set for convergence criteria for conservation of mass and momentum equation. First order upwind scheme along with SIMPLE algorithm for velocity pressure coupling is used to simulate the model. Table 3 depicts the details of grid independence study performed for aligned configuration for $H = 250 \mu m$ and $e = 25 \mu m$. The mesh quality super fine is used for the analysis.

Table 3 Details of grid independence study for aligned configuration, $H = 250 \mu m$ and $e = 25 \mu m$

Mesh Quality	Number of Nodes	Pressure Drop ($\frac{N}{m^2}$)
Very coarse	17331	876.12
Coarse	33747	846.13
Fine	62849	844.47
Super fine	123074	846.51
Finest	224959	846.304

The flow parameters are calculated in fully developed laminar region. To find fully developed length, pressure drop is extracted from each 1 mm length of the channel and pressure drop per unit length is calculated. After certain length from inlet the pressure drop per unit length becomes a constant value, which implies that fully developed condition has been reached. It is found that the flow becomes fully developed for a length 5 mm from the inlet for flow conditions. Hence length of fully developed region was selected as 7.5 mm for all calculation. Figure 3 depicts the variation of pressure drop per unit length for $H = 250 \mu m$, $\Phi = \frac{\pi}{2}$. The graph becomes asymptotic after 5 mm length of the channel for all Reynolds number, which indicates the flow has become fully developed. Further the pressure drop per unit length was found between any two arbitrary points within the fully developed region and this also gives the same value as $l = 7.5$ mm. This implies that the results are independent of the length of fully developed region. Figure 4 shows the developing and fully developed length of the flow domain.

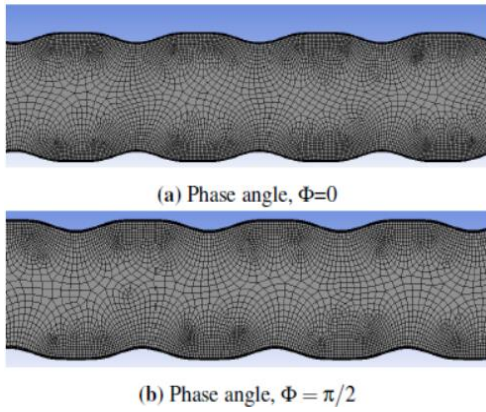


Fig. 2. Mesh generated for channel height $H = 250 \mu\text{m}$ and roughness height $e = 20 \mu\text{m}$.

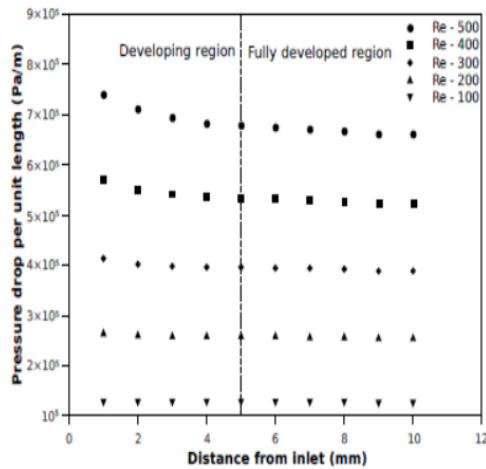


Fig. 3. Variation of pressure drop per unit length with distance from inlet ($H = 250 \mu\text{m}$, $\Phi = \pi/2$).

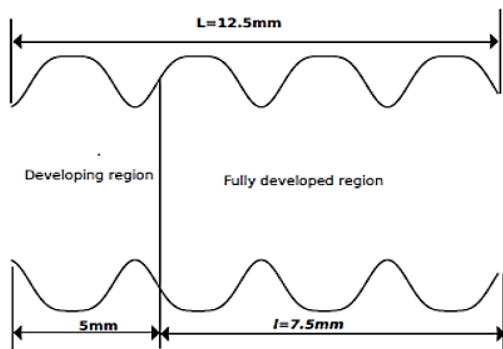


Fig. 4. Geometry showing length of fully developed region.

Constricted height of the channel is taken as characteristic length to define the flow field. Figure 1 shows the constricted height for different geometries. Since, the constricted height is a function of e , roughness height and Φ , phase angle, a new non-dimensional roughness parameter β is used to represent constricted height of the microchannel and is defined as

$$H_c = H - \lambda\beta \quad (5)$$

where β is defined by the equation

$$\beta = (1 + \cos^4 \Phi) \frac{e}{\lambda} \quad (6)$$

The definition of H_c is consistent with the definition of Wagner and Kandlikar (2012) used for aligned roughness pattern. For aligned roughness geometry $\Phi = 0$, H_c automatically reduces to $H_c = H - 2e$. But the definition for offset roughness ($\Phi = \pi/2$) is different from that of Koopaee and Zare (2015). They used the same definition for H_c as Wagner and Kandlikar (2012) for the analysis. In the present analysis for $\Phi = \pi/2$ the definition of constricted height reduces to $H_c = H - e$. However, this definition is in consensus with the geometry of the flow field.

The constricted parameter scheme proposed by Dharaiya and Kandlikar (2013) is used to define Reynolds number and friction factor of the flow and are defined in terms of constricted height as,

$$\text{Re} = \frac{\rho V H_c}{\mu} \quad (7)$$

$$f = \frac{2\Delta P H_c}{\rho l V^2} \quad (8)$$

where, l is length of fully developed region, V is velocity of the flow, ρ and μ are density and dynamic viscosity of water and H_c is constricted height of the channel. ΔP is pressure drop for length l .

RESULTS AND DISCUSSIONS

The numerical models are generated with specified geometric parameters defined in Table 2 and are meshed with commercial software ANSYS Fluent. The meshed models are simulated using prescribed boundary conditions, and the results are obtained from the converged solution. The 2D analysis of the models is carried out for different Reynolds number ranging from 100 to 500. The channels have a length of 12.5 mm and pitch is taken as height of the channel. The inlet velocity for different configurations is found from Eq. (7) and friction factor is calculated using Eq. (8).

Figures 5 and 6 represent the variation of pressure drop per unit length with Reynolds number for roughness height 5 μm for different channel height with phase angle 0 and $\pi/2$ respectively. It has been observed that as Reynolds number increases the pressure drop also increases for all configurations. The pressure drop is the highest for channel height 100 μm and the least for 250 μm . This may be due to when the channel height decreases the force needed to drive the flow increases; hence pressure drop per unit length also increases.

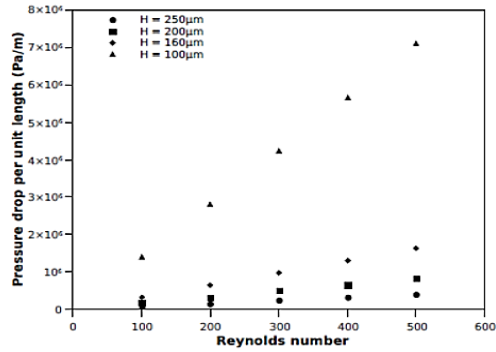


Fig. 5. Variation of pressure drop per unit length with Reynolds number $\Phi = 0, e = 5\mu\text{m}$.

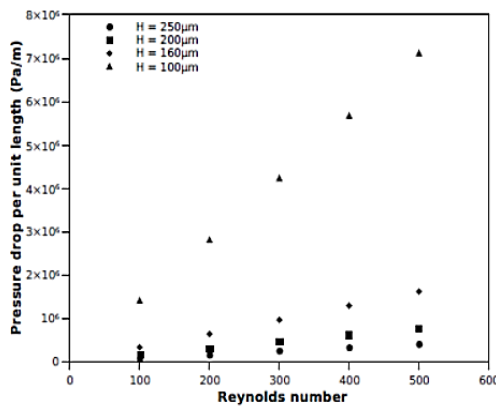


Fig. 6. Variation of pressure drop per unit length with Reynolds number ($\Phi = \pi/2, e = 5\mu\text{m}$).

The analysis revealed that for all channel heights the aligned pattern ($\Phi = 0$) gives higher pressure drop compared with offset configuration ($\Phi = \pi/2$) for the same roughness height and Reynolds number. Figure 7 depicts pressure drop variation with respect to Reynolds number for higher roughness heights. For small roughness height the difference is comparable, but as Reynolds number and roughness height increase the difference becomes much more prominent. This may be due to sudden contraction and expansion of the flow while passing through the aligned geometry. At high Reynolds number and roughness height, the loss due to sudden expansion and contraction is more significant whereas for small roughness height this kind of flow modification is almost negligible. When the phase angle increases from 0 to $\pi/2$ pressure drop decreases for all geometries. This may be due to when phase angle increases the constricted height of the channel increases and the velocity becomes more uniform. Figure 8 shows velocity contour for two extreme values of phase angle for channel height 250 μm and roughness height 30 μm at Reynolds number 500. Where, Fig. 8(a) shows velocity contour for aligned geometry ($\Phi = 0$) which confirms the variation in the velocity, while offset geometry ($\Phi = \pi/2$) in Fig. 8(b) shows a more uniform pattern. The uniform velocity variation in effect decreases the pressure drop per unit length. Koopae and Zare (2015) also reported similar flow behavior and pressure drop variation for aligned and offset configurations.

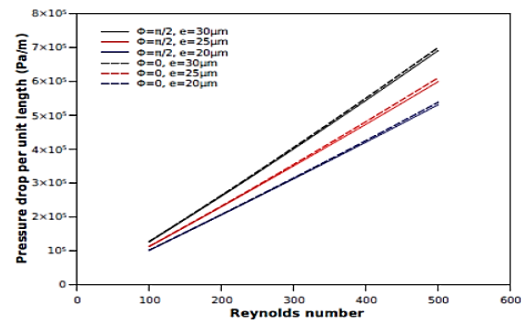
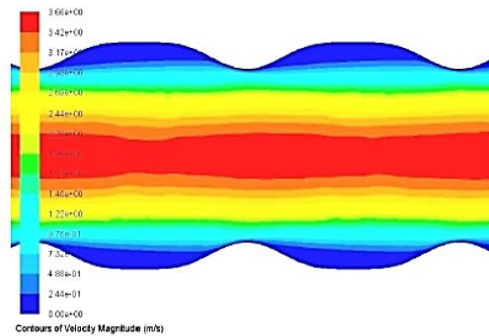
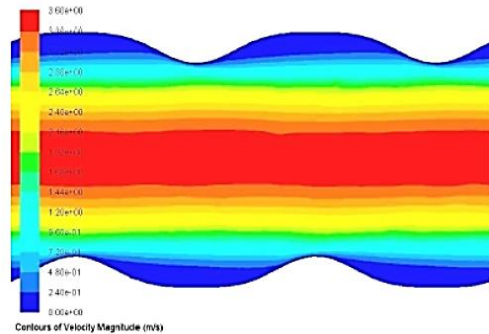


Fig. 7. Variation of pressure drop per unit length with Reynolds number ($H = 250\mu\text{m}$).



(a) Phase angle, $\Phi = 0$



(b) Phase angle, $\Phi = \pi/2$

Fig. 8. Velocity contour for $H = 250\mu\text{m}, e = 30\mu\text{m}, \text{Re} = 500$.

Even though the pressure drop per unit length is larger for aligned geometry, the maximum deviation with offset configuration is found to be 1.2% for channel height 250 μm roughness height 30 μm at Reynolds number 500. For low roughness values, the variation of pressure drop per unit length is insignificant for all configurations. This is due to the fact that at low roughness height the effect of phase angle on flow modification is almost negligible. Figures 9 and 10 show the variation of pressure drop per unit length with Reynolds number for channel height $H = 250\mu\text{m}$ at different phase angles. This depicts that the phase angle doesn't have any influence on pressure drop at low roughness heights.

Figures 11 and 12 show the variation of friction factor with Reynolds number for different channel heights and roughness height 5 μm . From the graph, it is clear that the friction factor decreases with Reynolds number for

all channel height. The offset pattern gives less flow resistance due to low pressure drop per unit length. The variation of friction factor is insignificant at lower roughness height for offset pattern, but aligned configuration shows much more deviation. Figure 13 shows the variation of friction factor for different phase angles with Reynolds number for channel height $H = 250 \mu\text{m}$ at different roughness height. It is observed that the variation of friction factor is insignificant at lower roughness height but shows considerable deviation as roughness height increases. This may be due to the modification of flow at higher roughness height as discussed earlier.

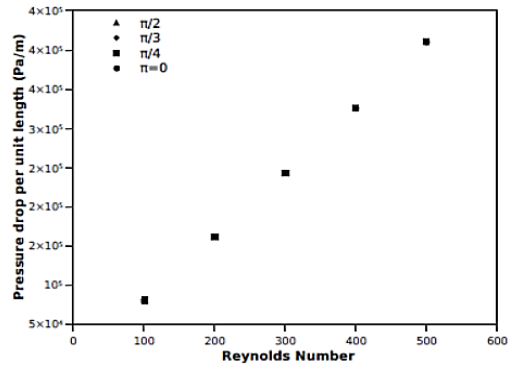


Fig. 9. Variation of pressure drop per unit length with Reynolds number for different Φ values ($H = 250 \mu\text{m}$, $e = 5 \mu\text{m}$).

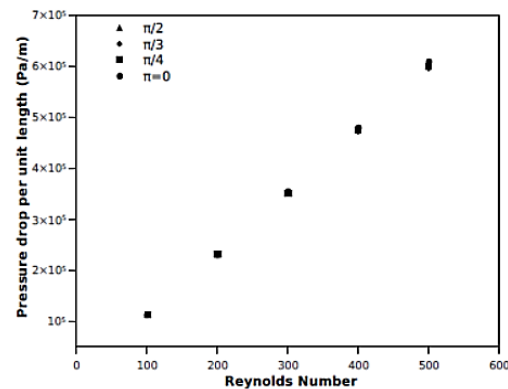


Fig. 10. Variation of pressure drop per unit length with Reynolds number for different Φ values ($H = 250 \mu\text{m}$, $e = 25 \mu\text{m}$).

Figure 14 represents the variation of friction factor for channel height $200 \mu\text{m}$. The friction factor doesn't show any variation with phase angle at relatively small roughness height $5 \mu\text{m}$. The same trend is observed for all other geometric configurations. Hence, it can be concluded from the numerical analysis that at low relative roughness, friction factor is independent of phase angle.

Based on the numerical analysis of models with different geometric parameters, a correlation for friction factor is developed as a function of Reynolds number and non-dimensional roughness parameter, β . The relation can be represented in a polynomial form as,

$$f = \frac{24}{\text{Re}} [1 + 0.156\beta - 86\beta^2 + 1691\beta^3 - 10764\beta^4 + 21352\beta^5] \quad (9)$$

where β is defined by the Eq. (6).

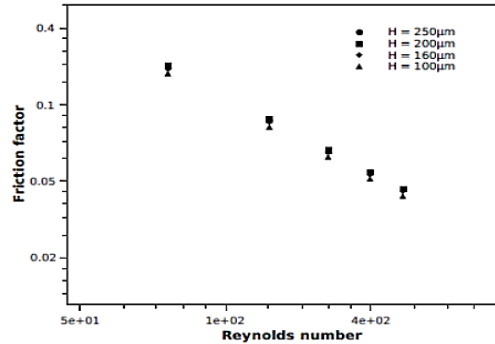


Fig. 11. Variation of friction factor with Reynolds number for different channel height ($\Phi = 0$, $e = 5 \mu\text{m}$).

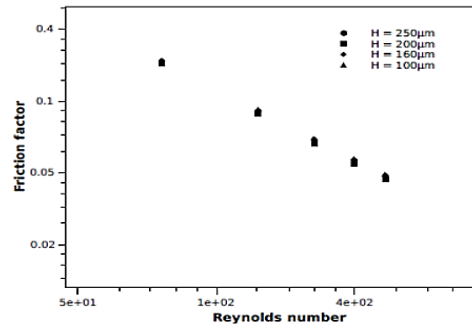


Fig. 12. Variation of friction factor with Reynolds number for different channel height ($\Phi = \pi/2$, $e = 5 \mu\text{m}$).

The correlation is valid for Reynolds number ranging from 100 to 500. The value of roughness parameter, β varies from 0.01 to 0.24. The Eq. (9) has a correlation coefficient of 0.99 and RMS error of $\pm 1.08\text{E-}02$ based on 220 data points. The terms in the polynomial are selected up to fifth degree, since adding one or more term doesn't improve the correlation significantly. The deviation between fifth and sixth-degree polynomial is less than 0.2%. Parity plot against correlation and numerical data is shown in Fig. 15 and maximum deviation is found to be 15% between the data. The validity of the correlation is tested with a random set of data that was not used to develop the correlation. A good agreement is found with Eq. (9) and is shown in Fig. 16. The validity of the correlation is further checked with the results presented in the literature.

The correlation is compared with the numerical result of Dharaiya and Kandlikar (2013) for Reynolds number 100 and is presented in Table 4. It is observed that the numerical friction factor presented by Dharaiya and Kandlikar (2013) and the value obtained from correlation is within the acceptable limit.

Table 4 Comparison of correlation with Dharaiya and Kandlikar (2013)

$H(\mu m)$	$\lambda(\mu m)$	$\lambda(\mu m)$	β	f , Dharaiya and Kandlikar (2013)	f , correlation	% deviation
550	250	10	0.08	0.2216	0.23425	5.4
550	250	16	0.128	0.2910	0.25443	14.37

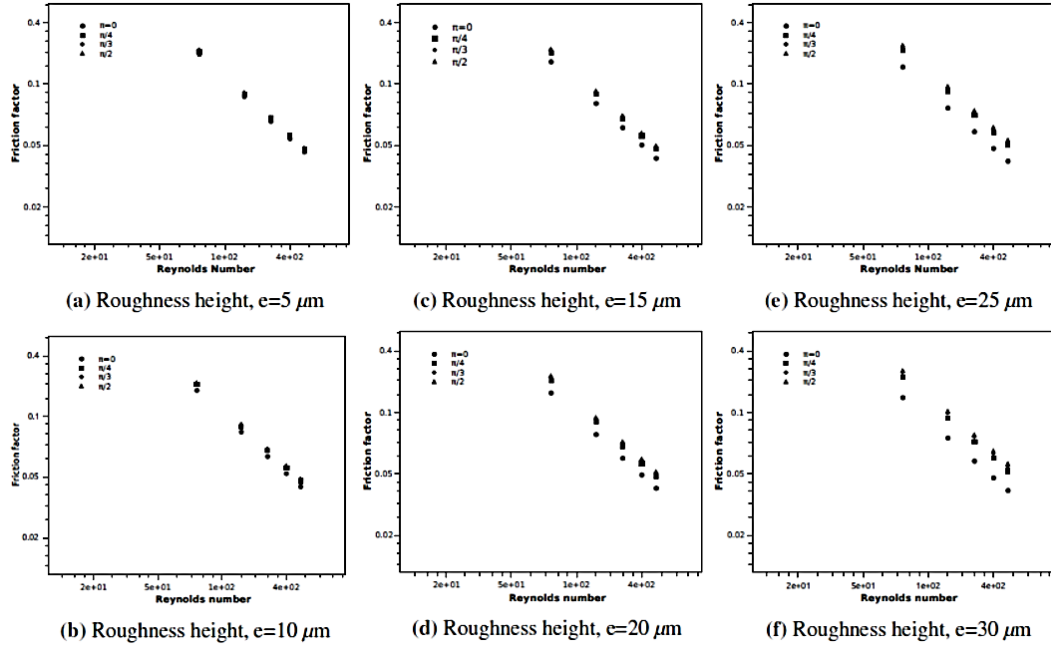


Fig. 13. Variation of friction factor with Reynolds number for $H = 250 \mu m$.

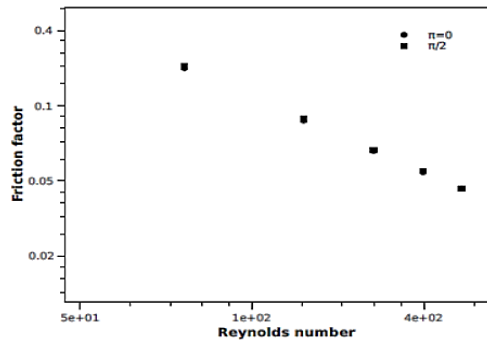


Fig. 14. Variation of friction factor with Reynolds number for $H = 200 \mu m$ and $e = 5 \mu m$.

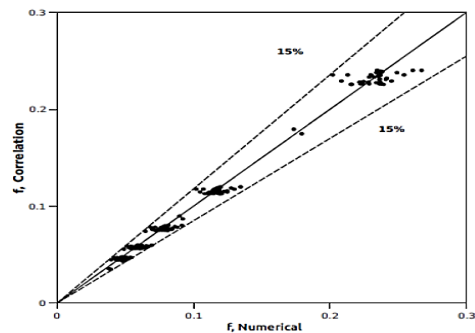


Fig. 15. Parity plot showing the goodness of correlation between Eq. (9) and numerical data.

Wagner and Kandlikar (2012) presented a wall function model for flow through rectangular microchannel. They have used sinusoidal function to generate the model and is validated with experimental and numerical data. The present correlation is compared with their experimental data set and is presented in Figs. 17 to 19.

Figure 17 shows the comparison of correlation with channel height $572 \mu m$ for $\beta = 0.0175$. Figure 18 represents the deviation of experimental friction factor and correlation for channel height $231 \mu m$ for $\beta = 0.0433$ and Fig. 19 for channel height $552 \mu m$ for $\beta = 0.0312$. The correlation value shows

reasonable agreement with experimental friction factor. The uncertainty reported for the measurement of Reynolds number and friction factor is 3.3% and 6.6% respectively.

The correlation is further compared with the result of Wu and Cheng (2003) and is found in good agreement with experimental friction factor. The experiments were performed with silicon trapezoidal microchannel with channel height $109.1 \mu m$ and for $\beta = 0.0302$. The measurement error reported for the calculation of friction factor is not more than 22.03%. The maximum error found between the correlation and experimental friction factor is 19%. Figure 20 depicts the comparison of values.

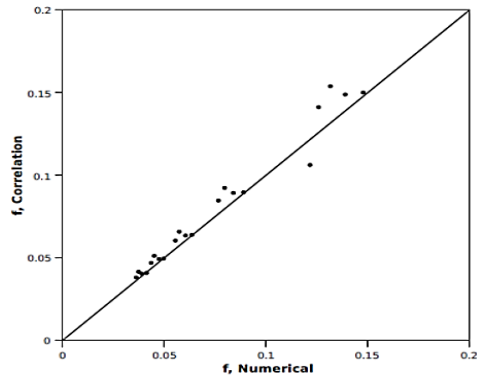


Fig. 16. Validation of correlation with numerical data not used to develop Eq. (9).

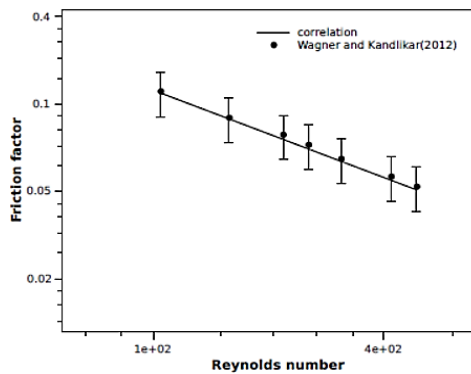


Fig. 17. Comparison of correlation with Wagner and Kandlikar (2012) for $H = 572 \mu\text{m}$ and $\beta = 0.0175$.

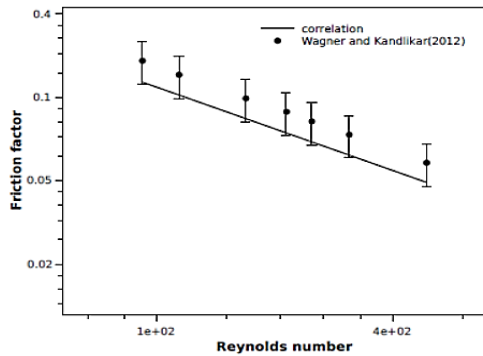


Fig. 18. Comparison of correlation with Wagner and Kandlikar (2012) for $H = 231 \mu\text{m}$ and $\beta = 0.0433$.

The validity of the Eq. (9) is checked with the experimental data obtained by [Steinke and Kandlikar \(2006\)](#). The data have been presented for the flow of deionized water through rectangular microchannel. The height of the channel is $244.2 \mu\text{m}$ and the value of roughness parameter, β is 0.01228. Figure 21 shows the comparison of experimental data with the correlation. The maximum deviation between the data is found to be 23%. According to Steinke and Kandlikar (2006), the uncertainty in measurement can be quite as large as 40%.

The roughness parameter used for validation of experimental data is defined by $\Phi = 0$, however Φ

can take any value between 0 and $\pi/2$. From the numerical analysis it is evident that at small roughness height, Φ has a nominal effect on friction factor and can be neglected. In most cases the average roughness of fabricated microchannel falls within this range. Hence one can choose the value of Φ conveniently as 0. It has been verified that the difference in friction factor between two extreme values of Φ used for analysis is only 1-2% and $\Phi = 0$ gives a better comparison with the experimental data presented in the literature. Also, if the value of roughness parameter is less than 0.01 the channel can be treated as smooth and can use the relation proposed by Kakac *et al.* (1987) to find the friction factor.

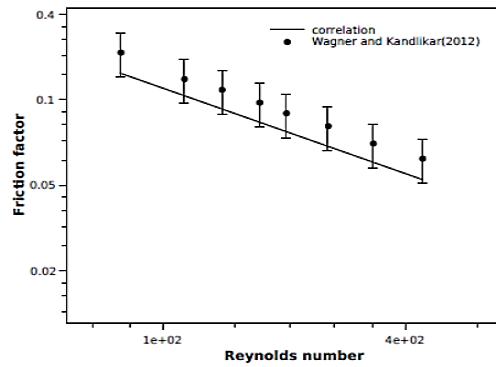


Fig. 19. Comparison of correlation with Wagner and Kandlikar (2012) for $H = 552 \mu\text{m}$ and $\beta = 0.0312$.

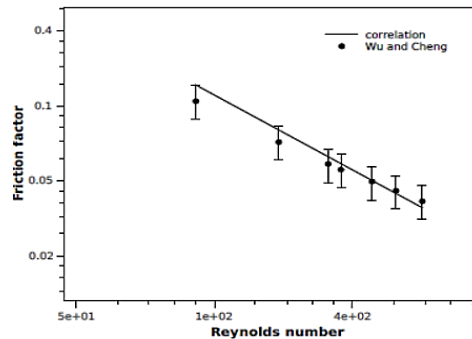


Fig. 20. Comparison of correlation with Wu and Cheng (2003) for $H = 109.1 \mu\text{m}$ and $\beta = 0.03$.

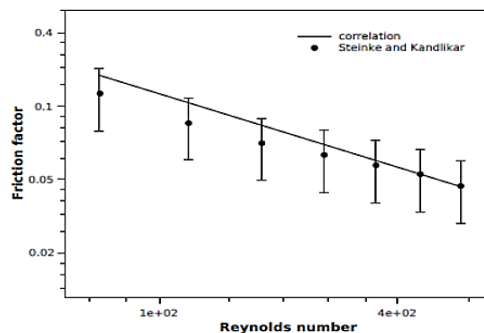


Fig. 21. Comparison of correlation with Steinke and Kandlikar (2006) for $H = 244.2 \mu\text{m}$ and $\beta = 0.01228$.

Table 5 Comparison of correlation with circular channel

Re	f , Li <i>et al.</i> (2007)	f correlation	%deviation	Re	f ,Mala and Li (1999)	f correlation	% deviation	Re	f , Li (2003)	f correlation	%deviation
102	0.6363	0.2222	186	117	0.5615	0.7936	190	330	0.1931	0.0686	181
260	0.2269	0.0882	157	165	0.4045	0.1383	192	490	0.1321	0.0465	184
360	0.1916	0.0629	204	265	0.2678	0.0861	211	575	0.1115	0.0392	184
403	0.1785	0.0562	217	350	0.2021	0.0646	213				
517	0.1486	0.0438	239	400	0.1803	0.0569	216				

The validity of the correlation is also checked with experimental data available in literature pertaining to flow through microtubes (Li (2003), Li *et al.* (2007) and Mala and Li (1999)) but found considerable deviation between the values. Table 5 shows the comparison of correlation with experimental data of circular microchannel. The experiments show that laminar fully developed flow through smooth circular microchannel obeys classical theory of fluid dynamics. For the present correlation, when the channel becomes smooth ($\beta \rightarrow 0$) the value of Poiseuille number becomes 24, whereas for circular channels it is 64. This may be a reason for the disparity between the values. Another reason may be the geometric parameters used for the analysis. The sinusoidal pattern for different Φ values may not be a good representative for the actual 3D rough surface of microtubes. The present geometry cannot be visualized as real 3D circular geometry for different Φ values because of its plane of symmetry. But these aspects need to be studied thoroughly to make a solid conclusion.

CONCLUSION

2D analysis of the flow of water through microchannel is performed by modeling structured sinusoidal rough surface with different geometric parameters. The simulation of the models was carried out using commercial software package ANSYS Fluent at optimum mesh quality. It is found that roughness height and Reynolds number have a significant effect on pressure drop and resistance to flow. The aligned cases of surface roughness give higher pressure drop for the same Reynolds number compared with offset configuration. It is observed that when the phase angle increases the pressure drop also increases. However, at low Reynolds number and roughness heights it is not so significant. The friction factor is also calculated at different Reynolds number and roughness heights. Based on the numerical analysis a correlation for friction factor is developed by introducing a new non-dimensional roughness parameter, β . The goodness of the correlation is checked with the numerical result and found less than 15% deviation between the data. The correlation is checked with data available in the literature within the limit specified and good agreement is observed. The correlation is valid for Reynolds number ranging 100 - 500 and β ranging

0.01 - 0.24. The correlation was also compared with experimental data pertaining to the circular microchannel and considerable deviation is observed.

ACKNOWLEDGEMENT

The work is supported by Center for Engineering Research and development, APJ Abdul Kalam Technological University (CERD-KTU), Kerala, India.

REFERENCES

Bein, A., W. Shin, S. Jalili-Firoozinezhad, M. H. Park, A. Sontheimer-Phelps, A. Tovaglieri, A. Chalkiadaki, H. J. Kim and D. E. Ingber (2018). Microfluidic organ-on-a-chip models of human intestine. *Cellular and molecular gastroenterology and hepatology* 5(4), 659–668.

Brackbill, T. P. and S. G. Kandlikar (2007). Effect of sawtooth roughness on pressure drop and turbulent transition in microchannels. *Heat transfer engineering* 28(8-9), 662–669.

Choi, S. B., R. F. Barron and R. O. Warrington (1991). Fluid flow and heat transfer in microtubes. *Micromech. Sensors, Actuators Syst.*, ASME DSC-32, 123.

Croce, G., P. Dagaró and C. Nonino (2007). Three-dimensional roughness effect on microchannel heat transfer and pressure drop. *International Journal of Heat and Mass Transfer* 50(25), 5249–5259.

Dharaiya, V. and S. Kandlikar (2013). A numerical study on the effects of 2d structured sinusoidal elements on fluid flow and heat transfer at microscale. *International journal of heat and mass transfer* 57(1), 190–201.

Ferreira, R. V., J. Sukumaran and P. De Baets (2011). Roughness measurement problems in tribological testing. In *Sustainable Construction and Design 2011* (SCAD), Volume 2, pp. 115–121. Ghent University, Laboratory Soete.

Guo, L., H. Xu and L. Gong (2015). Influence of wall roughness models on fluid flow and heat transfer in microchannels. *Applied Thermal*

- Engineering* 84, 399–408.
- Hao, P. F., Z. H. Yao, F. He, and K. Q. Zhu (2006). Experimental investigation of water flow in smooth and rough silicon microchannels. *Journal of Micromechanics and Microengineering* 16(7), 1397.
- Hsieh, S. S., C. Y. Lin, C. F. Huang, and H. H. Tsai (2004). Liquid flow in a micro-channel. *Journal of Micromechanics and Microengineering* 14(4), 436.
- Kakac, S., R. K. Shah, W. Aung, *et al.* (1987). *Handbook of single-phase convective heat transfer*. Wiley New York *et al.*
- Kandlikar, S. G., D. Schmitt, A. L. Carrano and J. B. Taylor (2005). Characterization of surface roughness effects on pressure drop in single-phase flow in minichannels. *Physics of Fluids* 17(10), 100606.
- Kim, B. (2016). An experimental study on fully developed laminar flow and heat transfer in rectangular microchannels. *International Journal of Heat and Fluid Flow* 62, 224–232.
- Koopae, K. M. and M. Zare (2015). Effect of aligned and offset roughness patterns on the fluid flow and heat transfer within microchannels consist of sinusoidal structured roughness. *International Journal of Thermal Sciences* 90, 9–23.
- Li, Z., Y. L. He, G. H. Tang and W. Q. Tao (2007). Experimental and numerical studies of liquid flow and heat transfer in microtubes. *International journal of heat and mass transfer* 50(17), 3447–3460.
- Li Zhi, X. (2003). Experimental study on flow characteristics of liquid in circular microtubes. *Microscale Thermophysical Engineering* 7(3), 253–265.
- Lin, T. Y., C. W. Chen, C. Y. Yang, and S. G. Kandlikar (2014). An experimental investigation on friction characteristics and heat transfer of air and CO₂ flow in microtubes with structured surface roughness. *Heat Transfer Engineering* 35(2), 150–158.
- Liu, Y., G. Xu, J. Sun and H. Li (2015). Investigation of the roughness effect on flow behavior and heat transfer characteristics in microchannels. *International Journal of Heat and Mass Transfer* 83, 11–20.
- Mala, G. M. and D. Li (1999). Flow characteristics of water in microtubes. *International journal of heat and fluid flow* 20(2), 142–148.
- Peiyi, W. and W. Little (1983). Measurement of friction factors for the flow of gases in very fine channels used for microminiature joule-thomson refrigerators. *Cryogenics* 23(5), 273–277.
- Pelević, N. and v. d. Meer and Th. H (2016). Heat transfer and pressure drop in microchannels with random roughness. *International journal of thermal sciences* 99, 125–135.
- Peng, X., G. Peterson and B. Wang (1994). Frictional flow characteristics of water flowing through rectangular microchannels. *Experimental Heat Transfer An International Journal* 7(4), 249–264.
- Pfahler, J., J. Harley, H. Bau and J. Zemel (1990). Liquid transport in micron and submicron channels. *Sensors and Actuators A: Physical* 22(1-3), 431–434.
- Pfund, D., D. Rector, A. Shekarriz, A. Popescu and J. Welty (2000). Pressure drop measurements in a microchannel. *AIChE Journal* 46(8), 1496–1507.
- Rawool, A., S. K. Mitra and S. Kandlikar (2006). Numerical simulation of flow through microchannels with designed roughness. *Microfluidics and nanofluidics* 2(3), 215–221.
- Sackmann, E. K., A. L. Fulton and D. J. Beebe (2014). The present and future role of microfluidics in biomedical research. *Nature* 507(7491), 181.
- Sahar, A. M., J. Wissink, M. M. Mahmoud, T. G. Karayiannis and M. S. A. Ishak (2017). Effect of hydraulic diameter and aspect ratio on single phase flow and heat transfer in a rectangular microchannel. *Applied Thermal Engineering* 115, 793–814.
- Steinke, M. E. and S. G. Kandlikar (2006). Single-phase liquid friction factors in microchannels. *International Journal of Thermal Sciences* 45(11), 1073–1083.
- Tuckerman, D. B. and R. Pease (1981). Highperformance heat sinking for vlsi. *IEEE Electron device letters* 2(5), 126–129.
- Wagner, R. N. and S. G. Kandlikar (2009). Mathematical model for fluid flow in artificially roughened microchannels. In *Proceedings of ASME 2009 International Mechanical Engineering Congress and Exposition, IMECE2009*, Nov, pp. 13–19.
- Wagner, R. N. and S. G. Kandlikar (2012). Effects of structured roughness on fluid flow at the microscale level. *Heat Transfer Engineering* 33(6), 483–493.
- Wang, H., Z. Chen and J. Gao (2016). Influence of geometric parameters on flow and heat transfer performance of micro-channel heat sinks. *Applied Thermal Engineering* 107, 870–879.
- Weaver, S., M. Barringer and K. Thole (2011). Microchannels with manufacturing roughness levels. *Journal of Turbomachinery* 133(4), 041014.
- White, F. (2011). *Fluid Mechanics. 7th edition McGraw Hill.*
- Whitesides, G. M. (2006). The origins and the future of microfluidics. *Nature* 442(7101), 368.
- Wu, H. and P. Cheng (2003). An experimental study

- of convective heat transfer in silicon microchannels with different surface conditions. *International Journal of Heat and Mass Transfer* 46(14), 2547–2556.
- Yu, D., R. Warrington, R. Barron and T. Ameel (1995). An experimental and theoretical investigation of fluid flow and heat transfer in microtubes. In *ASME/JSME Thermal Engineering Conference* 1, 523– 530.
- Zhai, Y., G. Xia, Z. Li and H.Wang (2017). Experimental investigation and empirical correlations of single and laminar convective heat transfer in microchannel heat sinks. *Experimental Thermal and Fluid Science* 83, 207–214.
- Zhang, C., Y. Chen and M. Shi (2010). Effects of roughness elements on laminar flow and heat transfer in microchannels. *Chemical Engineering and Processing: Process Intensification* 49(11), 1188– 1192.
- Zhuang, Q. C., N. Rui-Zhi, M. Yuan, and L. Jin-Ming (2016). Recent developments in microfluidic chip for in vitro cell-based research. *Chinese Journal of Analytical Chemistry* 44(4), 522–532.